Presence of base metals in the southern extension of Zawarmala Dolomite, Udaipur, Rajasthan, India

Ronak Jain

Department of Geology, Faculty of Earth Sciences,
Mohanlal Sukhadia University, Udaipur 313 001, India

This communication reports the presence of lead (Pb), zinc (Zn) and copper (Cu) mineralization in the dolomite rocks found in the southern part of the Zawarmala which is a well-known carbonate hosted Pb–Zn deposit occurring in the Zawar region in the south of Udaipur, Rajasthan, India. Remote sensing data analysis indicated the southern extension of the Zawarmala dolomite till Dhelai village where the outcrop truncates by the E–W fault. The carbonate with malachite strains supported by field evidences and petrological, ore microscopic, XRF and evidence of the presence of the trace elements reveal the presence of base metals in this area. The extension of occurrence of these dolomites rocks may be explored further for investigation of base metal mineralization in this region.

Keywords: ASTER, base metal, carbonates/dolomites, ore microscopy, trace elements, Zawarmala.

THE lead–zinc (Pb–Zn) bearing deposits present in the Aravalli Fold Belt of the Aravalli Craton and the carbonate hosted Pb–Zn belt of the Zawar range of Aravalli Supergroup are well known Pb–Zn deposit belt in Rajasthan. The present study lays emphasis on the rocks of the Palaeoproterozoic age of the Zawarmala belt of the Zawar deposit (Figure 1). The Zawarmala deposit is hosted by rocks of Zawar Formation equivalent to Mochia Formation of Middle Aravalli Group[1,2] (Table 1) or Baroi Magra Formation of Udaipur Group (Tiri Subgroup) of Aravalli Supergroup[3–5]. Geologically dolomite is the host rock for the Pb–Zn mineralization and the entire belt is bordered by Harn quartzites. Earlier workers explored the potentialities of Pb–Zn in the northern part of Zawarmala[6–13].

Remote sensing is one of the advanced technique that is highly utilized in the domain of geology for the identification and demarcation of the different lithologies and minerals[14–20]. The ASTER SWIR (short wave infrared) bands were utilized for the identification and mapping of the dolomites of the Zawarmala belt using the relative band depth (RBD) and a mineral map was derived using the formula ((band 6 + band 9)/band 8)[21,22] which demarcates the hydroxyl bearing (Mg–OH) minerals and carbonates (CO_3^{-2}). The geological boundary of the sulphide-bearing Mochia dolomite south of Zawaramala (after Gupta *et al.*[3]) was superimposed over the derived mineral map. The updated geological boundary of Mochia dolomite extends further south as two thin parallel belts and finally pinches off in phyllite and mica-schist of the Zawar Formation[3,4] of Aravalli Supergroup (Figure 2). Structural features of Zawaramala dolomites were demarcated using the false colour composite (R:4, G:6, B:8) overlain on the derived mineral map. The E–W and WNW–ESE trending faults were marked. The fault system is an important structural feature that is present in the Zawar region and is mainly responsible for the transportation of the Pb–Zn bearing hydrothermal fluid[6,8,12,13,23–25].

The dolomite is in general fine to medium-grained all along the southern extension of Zawarmala (Figure 3 *a* and *b*) with exceptions near the fault zones. Biotite is flaky and pleochroic from colourless to yellow and brown coloured mica present in the rocks. The cube-shaped opaques are scattered within the matrix of dolomite and quartz (Figures 3 *a* and *b*). Near the fault zones, the dolomite and quartz grains are elongated and the opaques are arranged parallel to them (Figure 3 *a* and *b*). The dolomite grain shape varies from anhedral to subhedral and the quartz grains are medium to fine grained with sutured contacts near Dhelai village. Gossan is present at this location which shows branching tree structures and

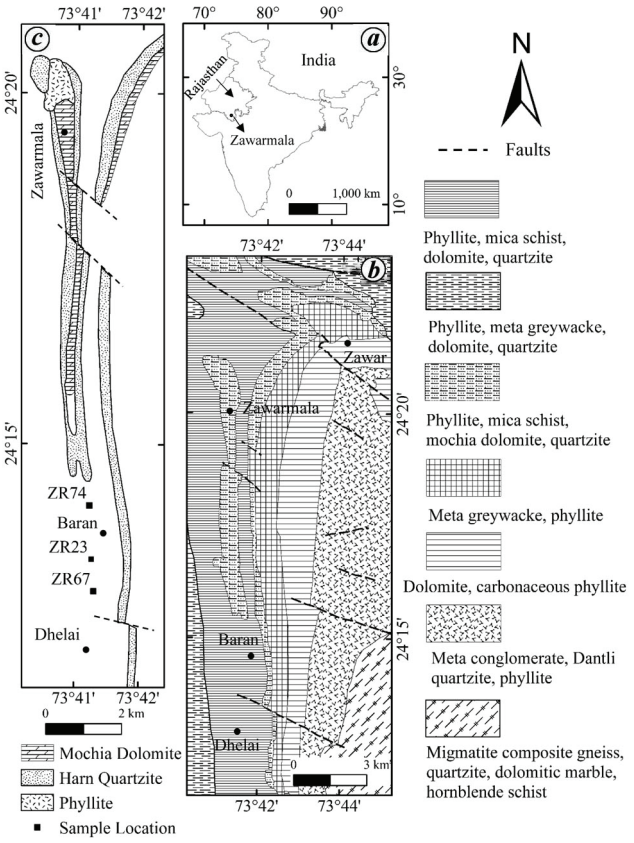

Figure 1. Geological map of the Zawarmala. ***a***, Inset map showing the location of Zawarmala in India. ***b***, Geological map around Zawar showing the extent of dolomites around Zawar and Zawarmala. ***c***, Lithological distribution map of the Zawarmala. Modified after Gupta *et al.*[3] and GSI[27].

e-mail: jainronak75@yahoo.in

Table 1. Stratigraphy sequence of the Aravalli Supergroup. Modified after Roy *et al.*[2,26] and Roy and Jakahr[1]

	Shelf sequences	
Upper Aravalli Group	Serpentinites (intrusions), Lakhawali Phyllite, Kabita Dolomite	
	Debari Fromation (= Dantalia Quartzite of Sarara inlier belt)	Quartzite-arkose-conglomerate
Middle Aravalli Group	Tidi Formation	Slate, phyllite with thin bands of dolomite and quartzite
	Bowa Formation = Machhala Magra Fromation	Quartzites and quartzose phyllite
	Mochia Formation = Zawar Formation[2]	Dolomite and facies variants, including carbonaceous phyllite with Pb, Zn, Ag
	Udaipur Formation = Kathalia Formation	Greywacke/phyllite, conglomerate
Lower Aravalli Group	Jhamarkotra Formation = Mandli Formation	Dolomite, quartzite, carbon phyllite, phyllite, thin local bands of stromatolitic phosphorite, copper and uranium deposits
	Delwara Formation	Metabasalt with thin bands of dolomite/quartz
Mewar Gneissic Complex		Pre-Aravalli gneisses, amphibolites, granitoids, metasediments

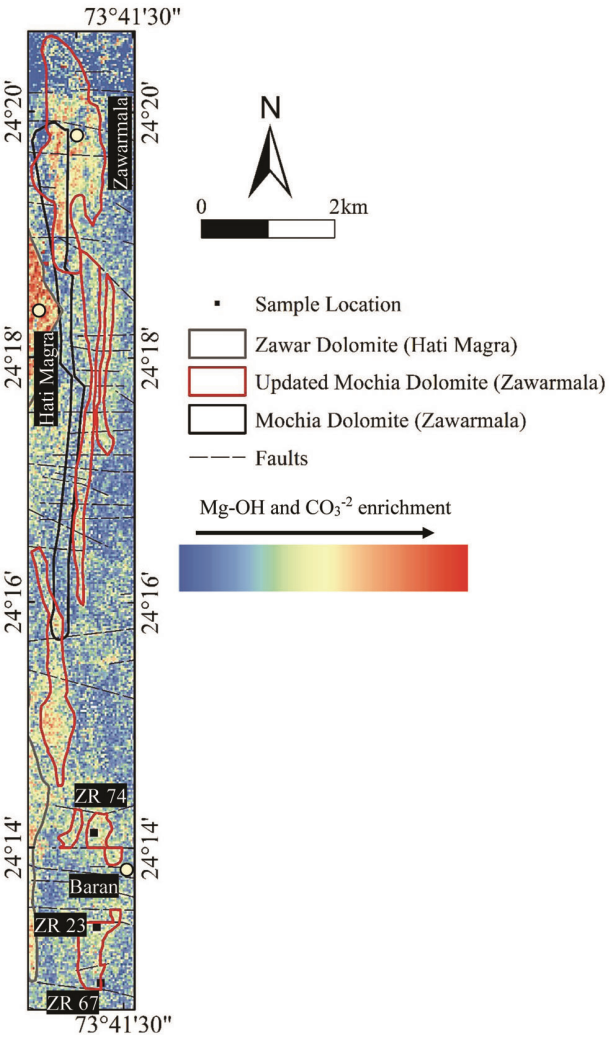

Figure 2. Relative band depth derived map from ASTER data showing the enrichment of the hydroxyl bearing (Mg–OH) and carbonate (CO_3^{-2}) minerals.

spheroid of iron oxide (Figure 3 *c* and *d*). Chlorite surrounds the gossan which imparts green colour in plane-polarized light. The Mochia dolomite is truncated by the E–W fault near the south of Dhelai village.

The opaque grains, i.e. mafics present in dolomite near Dhelai village were identified as galena and sphalerite by reflected light microscopy. Sphalerite imparts steel grey colour in plain polarized light whereas galena is grey

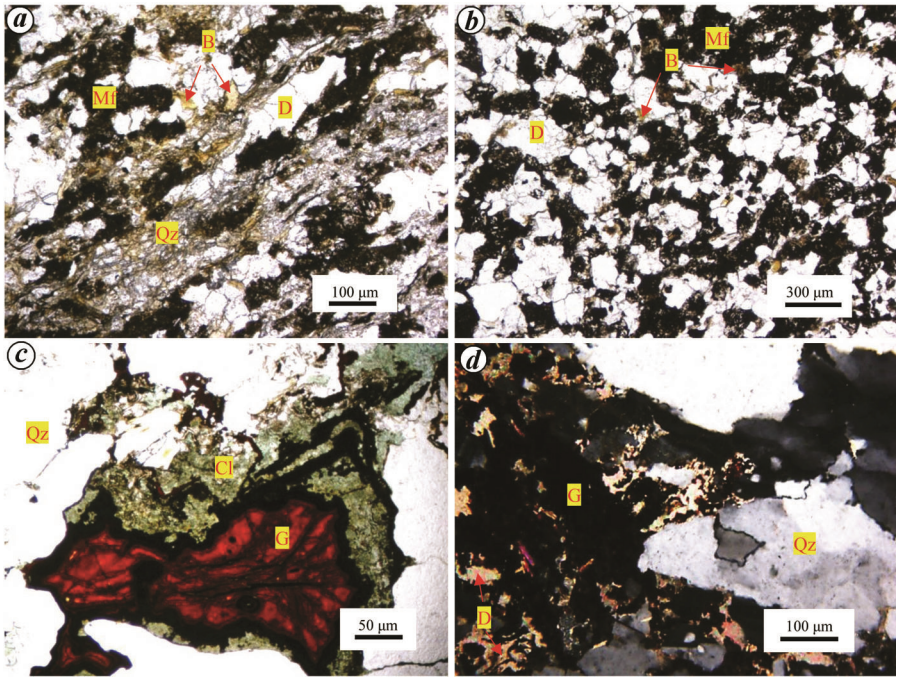

Figure 3. ***a***, Sheared dolomite with parallel arrangement of elongated grains of dolomite and quartz. Mafics are aligned along the longer axes (PPL). Location: Baran. ***b***, Fine to medium anhedral grained dolomite with biotite in the intergranular spaces (PPL). Location: Baran. ***c***, Concretions of iron oxide in gossan showing the spherical boundaries with tree branch pattern (PPL). Location: near Dhelai village. ***d***, Coarse-grained quartz with sutured grain contact in dolomite associated with opaques (XNicol). Location: near Dhelai village. D, Dolomite; B, biotite; Mf, mafics; Qz, quartz; Cl, chlorite and G, gossan.

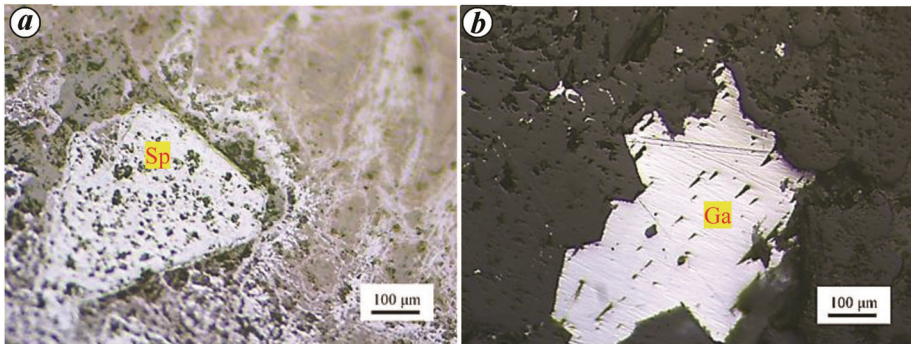

Figure 4. Photomicrographs of polished sections under reflected light. ***a***, Coarse-grained sphalerite in dolomite (PPL). Location: near Dhelai village. ***b***, Gray coloured triangular facet grains of galena (PPL). Location: near Dhelai village. Ga, Galena and Sp, Sphalerite.

Table 2. Major oxides (in weight %) of the selected samples from the southern extension of Zawarmala

Rock type	Sample no.	CaO	MgO	Na_2O	Al_2O_3	SiO_2	K_2O	Cr_2O_3	MnO	Fe_2O_3	Co_2O_3	NiO	CuO	ZnO	PbO
Dolomite	ZR 23	59.70	25.00	0.07	2.23	5.76	0.77	0.00	0.68	5.43	0.00	0.01	0.01	0.01	0.10
Dolomite	ZR 67(A)	24.10	9.02	0.12	2.71	56.80	1.07	0.00	0.43	5.34	0.00	0.01	0.01	0.00	0.01
Dolomite	ZR 67(B)	22.40	8.59	0.13	7.89	39.60	2.99	0.00	0.39	6.25	0.02	0.01	0.07	0.86	9.91
Dolomite	ZR 67(C)	8.20	0.89	0.25	17.15	51.80	4.33	0.00	0.22	9.51	0.14	0.03	6.35	0.24	0.20
Dolomite	ZR 74(E)	52.82	17.96	0.11	6.12	14.77	2.16	0.00	0.09	4.65	0.07	0.02	0.95	0.01	0.03

coloured and shows the characteristics features of triangular facets within the grain of galena (Figure 4).

The XRF and trace elemental analyses were conducted using the ZSX primus III+ Rigaku instrument at the Indian Institute of Technology (IIT), Bombay and Thermofisher Niton handheld XRF instrument respectively (Tables 2 and 3). The major oxides showed a higher concentration of CaO and MgO. In the sample ZR-67(C), lower concentration

Table 3. Trace elements (ppm) abundances of the selected samples from the southern extension of Zawarmala

Rock type	Sample no.	Cr	Mn	Fe	Co	Ni	Cu	Zn	Pb
Dolomite	ZR 23	0.0	5250.8	18989.7	0.0	94.3	79.1	55.4	928.3
Dolomite	ZR 67(A)	0.0	3306.9	18675.0	0.0	77.8	48.7	0.0	95.6
Dolomite	ZR 67(B)	0.0	3012.6	21857.4	76.4	58.1	560.8	6925.2	91996.1
Dolomite	ZR 67(C)	0.0	1711.5	33258.2	497.4	230.2	50728.2	1888.0	1865.9
Dolomite	ZR 74(E)	0.0	675.5	16279.2	259.7	126.6	7590.1	61.7	239.2

of MgO and higher CaO and SiO_2 along with the Al_2O_3, K_2O and Fe_2O_3 indicates the ferrous and siliceous nature of dolomite. The Pb, Zn and Cu oxides are present in these samples. The same has also been shown in the trace element analysis. The base metal elements like Pb, Zn and Cu are moderately concentrated in all samples but the samples ZR-67(B) and ZR-67(C) have a higher concentration of Pb and Cu and moderate concentration of Zn. The base metal concentration increases in iron and SiO_2 containing dolomites.

The southward extension of Zawarmala dolomite was identified using remote sensing technique which was confirmed by field studies and petrography. The reflected light microscopy confirmed the presence of galena and sphalerite in these dolomites. The major oxides and trace element concentration of the base metals (Pb, Zn and Cu) are significant in iron and silica-rich dolomites near fault zones compared to iron and silica devoid dolomites. These clues support to take up further base metal exploration in this region.

1. Roy, A. B. and Jakhar, S. R., *Geology of Rajasthan* (*Northwest India*)*: Precambrian to Recent*, Scientific Publishers (India), Jodhpur, 2002.
2. Roy, A. B., Paliwal, B. S., Shekhawat, S. S., Nagori, D. K., Golani, P. R. and Bejarniya, B. R., Stratigraphy of the Aravalli Supergroup in the type area. In *Precambrian of the Aravalli Mountain, Rajasthan, India* (ed. Roy, A. B.), Memoir of the Geological Society of India, 1988, pp. 121–131.
3. Gupta, S. N. *et al*., The Precambrian Geology of the Aravalli region, Southern Rajasthan and North-eastern Gujarat. *Mem. Geol. Surv. India*, 1997, **123**, 1–262.
4. GSI, *Geology and Mineral Resources of Rajasthan*, Miscellaneous Publication, No. 30, Part 12, Geological Survey of India, Western Region, India, 2011, 3rd edn.
5. Jain, R., Bhu, H. and Purohit, R., Application of thermal remote sensing technique for mapping of ultramafic, carbonate and siliceous rocks using ASTER data in Southern Rajasthan, India. *Curr. Sci.*, 2020, **119**, 954–961.
6. Roy, A. B. and Jain, A. K., Polyphase deformation in the Pb–Zn bearing Precambrian rocks of Zawarmala, Udaipur district, southern Rajasthan. *Q. J. Geol. Min. Metall. Soc. India*, 1974, **46**, 81–86.
7. Singh, N. N., *Structure and its bearing on the Sulphide Mineralization at Zawarmala (Zawar mines), Udaipur (Rajasthan), India*, University of Rajasthan, Jaipur, 1982.
8. Singh, N. N., Tectonic and stratigraphic framework of the lead-zinc sulphide mineralisation at Zawarmala, District Udaipur, Rajasthan. *J. Geol. Soc. India*, 1988, **31**, 546–564.
9. Vidyarthi, R. C. and Sen, R., Baroi–Zawarmala lead–zinc deposits, Zawar belt, Udaipur, Rajasthan, India. In Proceedings of Tectonics and Metallogeny of South and East Asia Geological Survey of India, Miscellaneous Publication No. 34, Calcutta, India, 1978, pp. 118–134.
10. Samar, M. S., Singh, N. N. and Hedge, M. P., Lead zinc mineralization in central part of Zawarmala, Zawar mines, Rajasthan. Abstract. In Discussion on Development for Basemetal (Copper-Lead-Zinc) deposits in Rajasthan and Gujarat, 1975.
11. Samar, M. S. and Singh, N. N., Geology and planned exploration of Zawarmala lead–zinc deposit. Abstract. In Indian Geological Congress, Udaipur, 1978, pp. 45–46.
12. Roy, A. B., Geometry and evolution of superposed folding in the Zawar lead–zinc mineralized belt, Rajasthan. *Proc. Indian Acad. Sci.* (*Earth Planet. Sci.*), 1995, **104**, 349–371.
13. Talluri, J. K., Pandalai, H. S. and Jadhav, G. N., Fluid chemistry and depositional mechanism of the epigenetic, discordant ores of the proterozoic, carbonate-hosted, Zawarmala Pb–Zn deposit, Udaipur District, India. *Econ. Geol.*, 2000, **95**, 1505–1525.
14. Jain, R., Kumar, A. and Sharma, R. U., Study of mineral mapping techniques: a case study in southeastern Rajasthan. In Proceedings of 38th Asian Conference on Remote Sensing – Space Applications: Touching Human Lives, ACRS Curran Associates, Inc., New York, New Delhi, India, 2017, pp. 2799–2807.
15. Jain, R., Kumar, A. and Sharma, R. U., *Study of Mineral Mapping Techniques using Airborne Hyperspectral Data: Exploring the Potential of AVIRIS-NG for Mineral Identification*, Lap Lambert Academic Publishing, Germany, 2018.
16. Jain, R. and Sharma, R. U., Airborne hyperspectral data for mineral mapping in Southeastern Rajasthan, India. *Int. J. Appl. Earth Obs. Geoinf.*, 2019, **81**, 137–145.
17. Guha, A., Chattoraj, S. L., Chatterjee, S., Vinod Kumar, K., Rao, P. V. N. and Bhaumik, K., Reflectance spectroscopy-guided broadband spectral derivative approach to detect glauconite-rich zones in fossiliferous limestone, Kachchh region, Gujarat, India. *Ore Geol. Rev.*, 2020, **127**, 103825.
18. Rani, K., Guha, A., Vinod Kumar, K., Bhattacharya, B. K. and Pradeep, B., Potential use of airborne hyperspectral AVIRIS-NG data for mapping proterozoic metasediments in Banswara, India. *J. Geol. Soc. India*, 2019, **95**, 152–158.
19. Guha, A., Yamaguchi, Y., Chatterjee, S., Rani, K. and Vinod Kumar, K., Emittance spectroscopy and broadband thermal remote sensing applied to phosphorite and its utility in geoexploration: a study in the parts of Rajasthan, India. *Remote Sensing*, 2019, **11**, 1003.
20. Jain, R. and Sharma, R. U., Mapping of mineral zones using the spectral feature fitting method in Jahazpur belt, Rajasthan, India. *Int. Res. J. Eng. Technol.*, 2018, **5**, 562–567.
21. Hewson, R. D., Cudahy, T. J., Mizuhiko, S., Ueda, K. and Mauger, A. J., Seamless geological map generation using ASTER in the Broken Hill-Curnamona province of Australia. *Remote Sensing Environ.*, 2005, **99**, 159–172.
22. Kalinowski, A. and Oliver, S., *ASTER Mineral Index Processing Manual*, Australia, 2004.
23. Straczek, J. A. and Srikantan, B., The geology of the Zawar lead–zinc area, Rajasthan, India. *Mem. Geol. Surv. India*, 1966, **92**, 1–85.
24. Smith, A. W., Remobilization of sulfide orebodies. *Econ. Geol.*, 1964, **59**, 930–935.

25. Poddar, B. C., Lead–zinc mineralization in the Zawar Belt, India – discussion. *Econ. Geol.*, 1965, **60**, 636–638.
26. Roy, A. B. *et al.*, Lithostratigraphy and tectonic evolution of the Aravalli Supergroup: a protogeosynclinal sequence. In *Rift Basins and Aulacogens* (ed. Casshyap, S. M.), Gyanodaya Prakashan, Nainital, 1993, pp. 73–90.
27. GSI, Udaipur Quadrangle. Geological Survey of India, 1999.

ACKNOWLEDGEMENTS. I thank the Space Applications Center, Indian Space Research Organisation, Ahmedabad, India for providing the financial support (EPSA/GHCAG/GSD/WP/15/2017) for the research. I acknowledge Dr Harsh Bhu for fruitful discussions on the initial draft of this paper and anonymous reviewers for suggesting the improvements in the manuscript. I also thank the Head, Department of Geology, M. L. Sukhadia University for providing the necessary research facilities.

Received 25 June 2021; revised accepted 17 August 2021

doi: 10.18520/cs/v121/i7/962-966

Increased xylanase activity in *Aspergillus niger* through mutation

Anjali Sharma[1], A. K. Jaitly[2,*] and Pankaj Kumar Rai[1]

[1]Department of Biotechnology, Invertis University, Bareilly 243 123, India
[2]Department of Plant Sciences, MJP Rohilkhand University, Bareilly 243 006, India

Aspergillus niger **is used for xylanase production on agricultural waste as substrate under broth culture. Rice straw and sugarcane bagasse have been the most potential substrate for xylanase production. Two different mutagens were used: UV radiation for different time durations and 5-bromouracil of different concentrations. Mutants so formed were selected on the basis of morphological and colony characteristics. Selected mutants were checked for their stability, requirement of amino acid and xylanase activity. Tested mutants showed 4-fold increase in xylanase activity from wild type.**

Keywords: Agricultural waste, mutation, rice straw, sugarcane bagasse, xylanase.

MICROBIAL enzymes are one of the fastest growing fields in biotechnology as these enzymes have several industrial applications[1]. Most common enzymes include cellulase, mannase, arabinase, xylanase, etc. Hemi-cellulose is the second most abundant renewable biomass in nature after cellulose. Xylan is the major hemi-cellulose component and accounts for 20–35% of plant cell wall dry weight[2]. Xylan provides potential raw materials for obtaining fermentable sugars which can be converted into several valuable products. Xylanases are hydrolytic enzymes which cleave the β-1,4 backbone of the hemi-cellulose. Xylanases and associated debranching enzymes are produced by a large variety of microorganisms including bacteria, actinomycetes, yeast and fungi[3].

Xylan consists of beta-1,4-linked D-xylopyranose as a backbone and short chains of o-acetyl, α-L-arabinofuranosyl, and α-D-glucuronyl residues. Enzymes such as endo-1,4-beta-xylanase, beta-D-xylosidase, beta-D-xylosidase, alpha-L-arabinofuranosidases, alpha-glucoronidases and acetyl esterases act synergistically to hydrolyse xylan. Pre-treatment with enzymes (mainly cellulase-free xylanase) has been reported as an environmentally benign and less expensive[4] method that aids in the spread of hardwoods and softwoods[5].

Enzymatic conversion of hemi-cellulose produces high value products like furfural, xylitol, biofuels and in artificial low calorie sweeteners[6]. Breakdown of hemicelluloses in wheat flour makes the dough softer and easier to knead[7]. Micro-organisms such as bacteria and fungi producing xylanases are more favoured as they are easily available and structurally stable as well as can also be easily genetically manipulated. It has been reported that fungi are more efficient in producing xylanase in comparison to bacteria, however some species of *Bacillus* have been reported to secrete important extracellular enzymes and protein in the medium.

Mutation plays an important role in improving fungal strains for specific work. Mutation may take place spontaneously or may be induced. Spontaneous mutation is slow and their rate depends on the growth conditions of organism and the mutation frequency is low[8]. Induced mutation could be carried out either by physical or chemical methods. Physical mutation could be carried out by UV radiation, gamma radiation or X-rays[9] whereas the chemical mutation is carried out using EtBr (ethidium bromide), 5-bromouracil, EMS (ethyl methyl sulphonate), etc. Xylanase activity of *A. niger* has been increased up to 118% by mutation. UV radiation has been reported as very effective in industries and do not require any equipment. As a result, the current study aims to increase xylanase activity in *A. niger* by mutation in order to investigate its industrial potential[10]. As it has been reported that xylanase is produced by different *Aspergillus* species such as *A. nidulans*, *A. niger* and *A. oryzae*. Different strains of *A. niger* have been reported for the production of Xylanase through mutagenesis. Mutagenesis involves two different methods which includes physical and chemical; in the physical method fungus is treated with UV radiations for different time intervals and in the chemical method fungus is grown on the medium containing chemical mutagen such as 5-bromouracil, ethylmethyl sulphonate, etc. In the commercial development of microbial fermentation processes, industrial strain enhancement is critical. According to Rowlands[11], mutagenic methods can be tweaked in

*For correspondence. (e-mail: jaitly1958@gmail.com)